# The EPAC–Rap1 pathway prevents and reverses cytokine-induced retinal vascular permeability

Received for publication, August 31, 2017, and in revised form, November 15, 2017 Published, Papers in Press, November 20, 2017, DOI 10.1074/jbc.M117.815381

Carla J. Ramos, Chengmao Lin, Xuwen Liu, and David A. Antonetti[1]

*From the Department of Ophthalmology and Visual Sciences, University of Michigan, Kellogg Eye Center, Ann Arbor, Michigan 48105*

Edited by Karen G. Fleming

**Increased retinal vascular permeability contributes to macular edema, a leading cause of vision loss in eye pathologies such as diabetic retinopathy, age-related macular degeneration, and central retinal vein occlusions. Pathological changes in vascular permeability are driven by growth factors such as VEGF and pro-inflammatory cytokines such as TNF-$\alpha$. Identifying the pro-barrier mechanisms that block vascular permeability and restore the blood–retinal barrier (BRB) may lead to new therapies. The cAMP-dependent guanine nucleotide exchange factor (EPAC) exchange-protein directly activated by cAMP promotes exchange of GTP in the small GTPase Rap1. Rap1 enhances barrier properties in human umbilical endothelial cells by promoting adherens junction assembly. We hypothesized that the EPAC–Rap1 signaling pathway may regulate the tight junction complex of the BRB and may restore barrier properties after cytokine-induced permeability. Here, we show that stimulating EPAC or Rap1 activation can prevent or reverse VEGF- or TNF-$\alpha$–induced permeability in cell culture and *in vivo*. Moreover, EPAC activation inhibited VEGF receptor (VEGFR) signaling through the Ras/MEK/ERK pathway. We also found that Rap1B knockdown or an EPAC antagonist increases endothelial permeability and that VEGF has no additive effect, suggesting a common pathway. Furthermore, GTP-bound Rap1 promoted tight junction assembly, and loss of Rap1B led to loss of junctional border organization. Collectively, our results indicate that the EPAC–Rap1 pathway helps maintain basal barrier properties in the retinal vascular endothelium and activation of the EPAC–Rap1 pathway may therefore represent a potential therapeutic strategy to restore the BRB.**

The retinal vasculature provides oxygen and nutrients to the inner retina and forms the inner blood-retinal barrier (iBRB)[2] that helps maintain the retinal environment, allowing for proper neural function (1). The BRB maintains strict regulation of vascular permeability through a continuous endothelium lacking fenestrations, has limited transcellular vesicles, and controls the flux through the intercellular spaces between endothelial cells through the formation of a well developed junctional complex (2, 3).

Tight junctions (TJs) promote endothelial cell barrier properties by restricting the passage of molecules through the intercellular space (gate function) and conferring cell polarity by preventing lateral diffusion of lipids and proteins in the plasma membrane (fence function) (4). Over 40 proteins make up the TJs that are subdivided into transmembrane and scaffolding proteins (5). Important retinal endothelial cell transmembrane proteins include, but are not limited to, occludin and claudin-5 along with scaffolding proteins zonula occludens, ZO-1, -2, and -3, which connect the TJ to the actin cytoskeleton. Eye pathologies that result from elevated levels of permeabilizing agents such as vascular endothelial growth factor (VEGF) and pro-inflammatory cytokines like TNF-$\alpha$ exhibit increased retinal vascular permeability, which occurs at least in part by disrupting TJ organization (6). TJ disruption may be mediated by VEGF-induced occludin phosphorylation (7), or TNF-$\alpha$–induced reduction in claudin-5 and ZO-1 expression (8) as well as currently uncharacterized mechanisms. Current medical therapies for macular edema involve intraocular injection of anti-VEGF agents, which demonstrate good effectiveness in approximately half of treated patients (9).

The second messenger cAMP regulates several cell signaling pathways including barrier properties in endothelial cells (10, 11). In addition to the well studied cAMP effector protein kinase A (PKA) an additional cAMP effector was identified, named exchange-protein-directly activated by cAMP (EPAC) (12). This exchange factor targets the small GTPase, Ras-associated protein (Rap), promoting exchange of GDP for GTP and activation of Rap (13). Mammals express two isoforms of the EPAC protein, EPAC1 (RapGEF3), which is widely expressed, and EPAC2 (RapGEF4), which is prominently expressed in the brain and adrenal gland (14). The Rap proteins are small GTPases in the Ras family involved in several cell-signaling

This work was supported by National Institutes of Health Grant EY012021 (to D. A. A.), grants from the Research to Prevent Blindness (to D. A. A.) and Kellogg Eye Center Core Center for Vision Research, National Institutes of Health Grant P30EY007003, and Michigan Diabetes Research and Training Center Grant DK020572. The authors declare that they have no conflicts of interest with the contents of this article. The content is solely the responsibility of the authors and does not necessarily represent the official views of the National Institutes of Health.

This article contains Figs. S1–S6.

[1] To whom correspondence should be addressed: Kellogg Eye Center, 1000 Wall St., Ann Arbor, MI 48105. Tel.: 734-232-8230; Fax: 734-232-8030; E-mail: dantonet@med.umich.edu.

[2] The abbreviations used are: iBRB, inner blood-retinal barrier; EPAC, exchange-protein-directly activated by cAMP; TJ, tight junctions; 8-CPT-2′-*O*-Me-cAMP, 8-(4-chloro-phenylthio)-2′-*O*-methyl-cAMP; 8-CPT-AM, 8-CPT-2-*O*-Me-cAMP-acetoxymethyl; HUVEC, human umbilical vein endothelial cell; IR, ischemia reperfusion; RPE, retinal pigment epithelium; BREC, bovine retinal endothelial cell; RITC, rhodamine isothiocyanate; CREB, cAMP-response element-binding protein; TEER, transendothelial electrical resistance; qRT, quantitative RT; RBD, Rho-binding domain; GTPγS, guanosine 5′-3-*O*-(thio)triphosphate; FSK, forskolin.

mechanisms. Mammals express two Rap proteins from separate genes, Rap1 and Rap2, which share ~60% protein sequence homology (15, 16). Rap1 is further divided into two highly homologous isoforms, Rap1A and Rap1B, which are encoded by different genes (17). Rap2 has three isoforms (Rap2A, Rap2B, and Rap2C) and their functions have not been well characterized (18). Vascular development requires Rap1 proteins, as vasculature conditional gene deletion of both *Rap1A* and *Rap1B* leads to complete embryonic lethality by E15.5 (19). Interestingly, mice with *Rap1A* deleted and only one *Rap1B* allele are viable, whereas mice with *Rap1B* deleted and only one *Rap1A* allele are not, suggesting a critical role for Rap1B in endothelial vasculature (19). Active Rap1 proteins are known for their role in cell adhesion in leukocytes (20) and cell adherens junction regulation (21). However, the relationship of Rap to TJs is not well understood.

The development of EPAC-specific cAMP analogs, such as 8-(4-chloro-phenylthio)-2′-O-methyladenosine-3′,5′-cyclic monophosphate (8-CPT-2′-*O*-Me-cAMP) and the improved membrane permeable 8-CPT-2′-*O*-Me-cAMP-AM (8-CPT-AM), which contains an acetoxymethyl group (AM) to mask the negative charge from the phosphate group, has allowed investigation of the cAMP—EPAC–Rap1 pathway independent of PKA signaling. Studies focusing on the activation of EPAC–Rap1 signaling in endothelial cells such as human umbilical vein endothelial cells (HUVEC) have identified a role for EPAC/Rap in regulating barrier properties through a cortical actin increase at the endothelial junctions (22), recruitment of junctional proteins such as VE-cadherin (23), and inhibition of the small GTPase, RhoA, known to be involved in permeability (24). However, very little is known about the role of the EPAC–Rap1 signaling pathway in endothelial cells that form barriers of the CNS such as the BRB.

In the present study, we demonstrate a role for the EPAC–Rap1 signaling pathway in retinal vascular endothelial cells. We show Rap1B confers basal barrier properties to retinal endothelial cells and that pharmacologic activation of the EPAC–Rap1 pathway can prevent and restore BRB properties after both growth factor- and inflammatory factor-induced permeability. Furthermore, activation of EPAC–Rap1 signaling is shown to promote TJ organization and reduce paracellular permeability.

## Results

### *Activation of EPAC prevents VEGF- and TNF-α–induced permeability and reverses ischemia reperfusion-induced permeability in vivo*

Activation of the EPAC–Rap1 signaling pathway via the EPAC-specific cAMP analog, 8-CPT-2′-*O*-Me-cAMP, regulates barrier properties in endothelial cells such as HUVEC, pulmonary endothelial cells, and in rat mesenteric microvasculature (24–26). However, little is known about the role of EPAC–Rap1 signaling in the endothelial cells of the BRB or the relationship of EPAC–Rap1 signaling to vascular permeabilizing factors such as VEGF and TNF-α. Long-Evans rats were utilized to determine whether pharmacological activation of the EPAC–Rap1 signaling pathway prevents retinal vascular permeability *in vivo*. First, to determine the localization of *Rap1* expression in retinas, immunofluorescent staining of rat retinas was performed using an anti-Rap1 antibody, which binds both the Rap1A and -B isoforms; retinas were co-stained with IB4 to identify blood vessels. Rap1 was located only in the capillary vessels and colocalizes with IB4 staining (Fig. 1*A*). Next, VEGF and TNF-α were intravitreally co-injected into Long-Evans rats and 3 h later, Evan's Blue was administered through the femoral vein to assess Evan's Blue dye accumulation in the retina tissue as a measure of retinal vascular permeability. VEGF and TNF-α increased retinal vascular permeability by 2-fold in comparison to control (Fig. 1*B*). The retinas that were intravitreally co-injected with either 10 or 50 μM 8-CPT-AM, along with both VEGF and TNF-α, had no significant increase in retinal vascular permeability compared with controls, showing that 8-CPT-AM treatment blocks VEGF/TNF-α–induced permeability (Fig. 1*B*). To determine whether activation of the EPAC–Rap1 signaling pathway can restore barrier properties to the retinal vasculature, an ischemia reperfusion model was used. In rodent models, ischemia reperfusion (IR) rapidly induces a VEGF-dependent increase in retinal vascular permeability, which persists for at least 48 h and leads to expression of a host of inflammatory factors (27). IR was induced in mice and 48 h later, 8-CPT-AM was administered intravitreally and retinal vessel permeability was compared with vehicle-injected control eyes. The 100 μM 8-CPT-AM concentration used for intravitreal injection was a dose shown to activate EPAC independent of PKA activation in retinal pigment epithelium (RPE) and choroid (28, 29) and was shown to not increase PKA activity (Fig. S1*A*). Animals with ischemia displayed a 2-fold increase in retinal vascular permeability (Fig. 1*C*), as previously observed in rat (27). Mice that received intravitreal injection of 100 μM 8-CPT-AM after ischemia showed a reversal of ischemia-induced retinal vascular permeability by measuring accumulation of FITC-BSA (Fig. 1*C*) or 70-kDa dextran-Texas Red in the retina (Fig. S1*B*).

### *Activation of the EPAC–Rap1 pathway prevents and reverses VEGF- or TNF-α–induced endothelial permeability*

The EPAC–Rap1 signaling pathway in VEGF- or TNF-α–induced endothelial permeability was examined in primary culture of bovine retinal endothelial cells (BREC). Western blotting reveals that EPAC and Rap1 proteins are expressed in BREC (Fig. 2*A*). To validate that 8-CPT-AM activates the EPAC–Rap1 signaling pathway in these cells, we used the active Rap1 capture assay, which captures active, GTP-bound Rap1 through binding to a GST-linked peptide for the downstream Rap1 effector RalGDS. Confluent monolayers of BREC were treated with VEGF, or first pretreated with 8-CPT-AM then VEGF or 8-CPT-AM alone, and compared with controls. BREC treated with 8-CPT-AM (1 μM) showed a significant 2.5-fold increase in Rap1 bound to GTP. One hour of VEGF had no apparent effect on Rap1 GTP loading with or without 8-CPT-AM (Fig. 2, *B* and *C*). To determine whether longer exposure of VEGF affected the ability of 8-CPT-AM to induce Rap1 GTP loading, BREC were stimulated with VEGF for 24 h followed by 30 min of 8-CPT-AM (1 μM). Longer exposure of VEGF had no effect on Rap1 GTP loading and again 8-CPT-AM alone or after VEGF induced a significant 2–3-fold increase

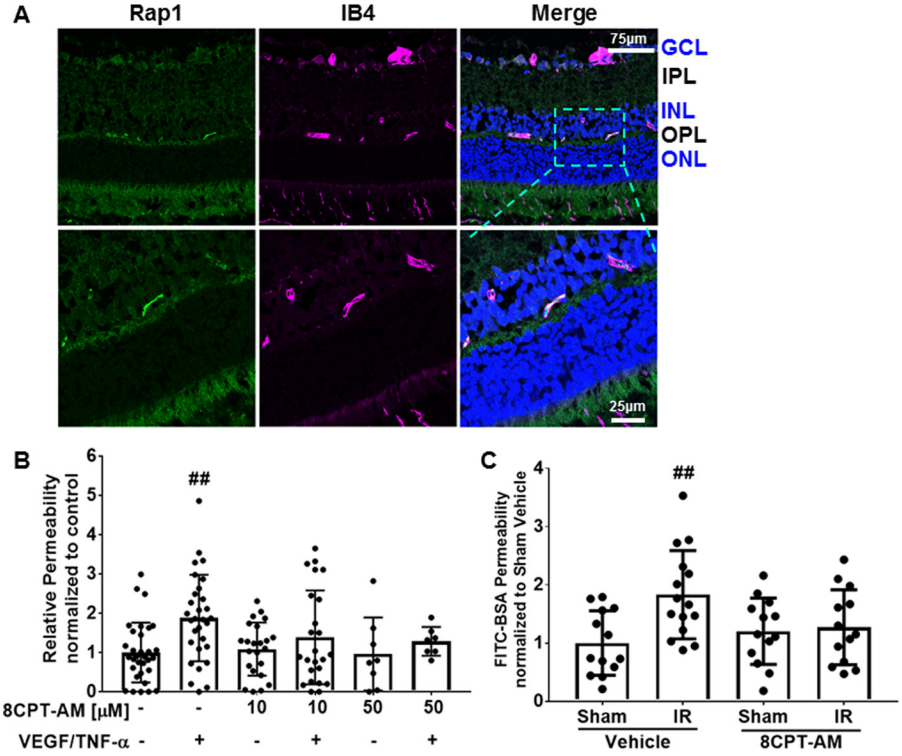


**Figure 1. Cyclic AMP analog, 8-CPT-AM, regulates retinal vascular permeability.** *A,* Rap1 is found in the capillary plexus of the retina. Immunofluorescence analysis was utilized to detect the presence of Rap1 (*green*) in rat retina. IB4 vascular marker (*purple*) and Hoechst nuclear stain was used. Ganglion cell layer (*GCL*), inner nuclear layer (*INL*), outer plexiform layer (*OPL*), outer nuclear layer (*ONL*) are shown. *Scale bars*, 75 and 25 $\mu$m for zoom images. *B,* 8-CPT-AM blocks retinal vascular permeability. Long-Evans rats received intravitreal co-injection of VEGF (50 ng) and TNF-$\alpha$ (10 ng) or 8-CPT-AM at 355 ng (an estimated vitreous concentration of 10 $\mu$M) or 1.78 $\mu$g (estimated 50 $\mu$M) with VEGF and TNF-$\alpha$ and compared with vehicle control. After 3 h, rats received a femoral vein injection of Evan's Blue and retinal dye accumulation was determined. *C,* 8-CPT-AM reverses ischemia reperfusion-induced permeability. Retinal ischemia in mice was achieved by increasing the intraocular pressure with PBS delivered to the anterior chamber to prevent blood flow for 90 min followed by natural reperfusion. 48 h later vehicle or 8-CPT-AM at 278 ng (estimated vitreous concentration of 100 $\mu$M) was delivered by intravitreal injection and FITC-BSA dye accumulation was determined. Results are expressed as the mean relative to the control ± S.D., Bonferroni post hoc test, ##, $p < 0.01$ compared with control.

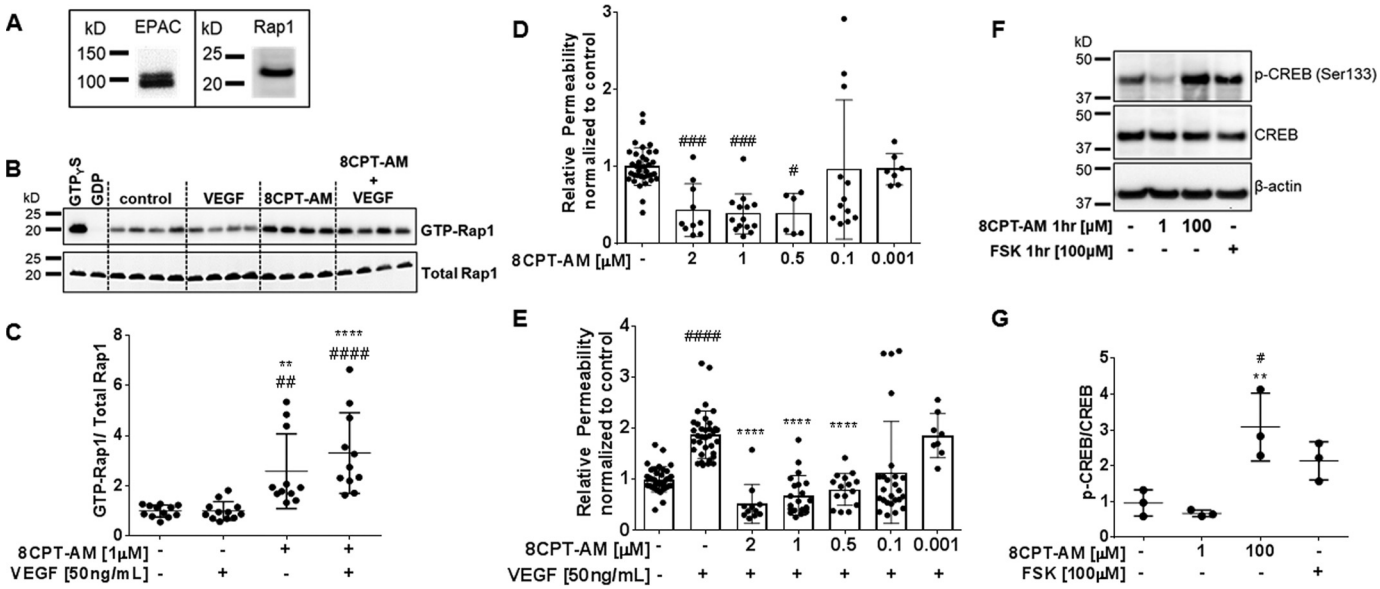


**Figure 2. 8-CPT-AM Rap1 activation prevents VEGF-induced permeability of BREC.** *A,* Western blot analysis from BREC lysates shows the presence of the GEF EPAC1 and small G-protein Rap1. *B,* GTP bound Rap1 was determined by capture assay using GST-RalGDS RBD. 8-CPT-AM (1 $\mu$M) was added 30 min prior to VEGF (50 ng/ml) for a total time of 1.5 h. Assay controls GTP$\gamma$S and GDP were added to lysates before capture. Quantification is shown in *C* with a total $n \geq 11$. *D,* solute flux assay was used to test permeability to 70-kDa RITC-dextran after 8-CPT-AM at varying concentrations on BREC, $n \geq 6$. *E,* 8-CPT-AM prevents VEGF-induced permeability. BREC stimulated with 8-CPT-AM at the doses indicated are 30 min prior to VEGF addition. Doses from 0.5 to 2 $\mu$M blocked VEGF-induced permeability. Average $P_o$ values for control were $7.1 \times 10^{-7}$ and VEGF were $1.4 \times 10^{-6}$ (cm/s), total of $n \geq 8$. *F,* low dose 8-CPT-AM does not activate the PKA pathway. 8-CPT-AM at 1 $\mu$M was added to BREC for 1 h and no increase in CREB phosphorylation was observed. Incubation of 8-CPT-AM or forskolin (*FSK*) at 100 $\mu$M for 1 h increased CREB phosphorylation. *G,* quantification shown in *F* with a total $n \geq 3$. All results are expressed as the mean ± S.D. relative to the control. One-way ANOVA and Bonferroni post hoc test: #, $p < 0.05$; ##, $p < 0.01$; ###, $p < 0.001$; ####, $p < 0.0001$ compared with control in *C–E* and *G*. **, $p < 0.01$; ****, $p < 0.0001$ compared with VEGF in *C* and *E* or 8-CPT-AM (1 $\mu$M) in *G*.

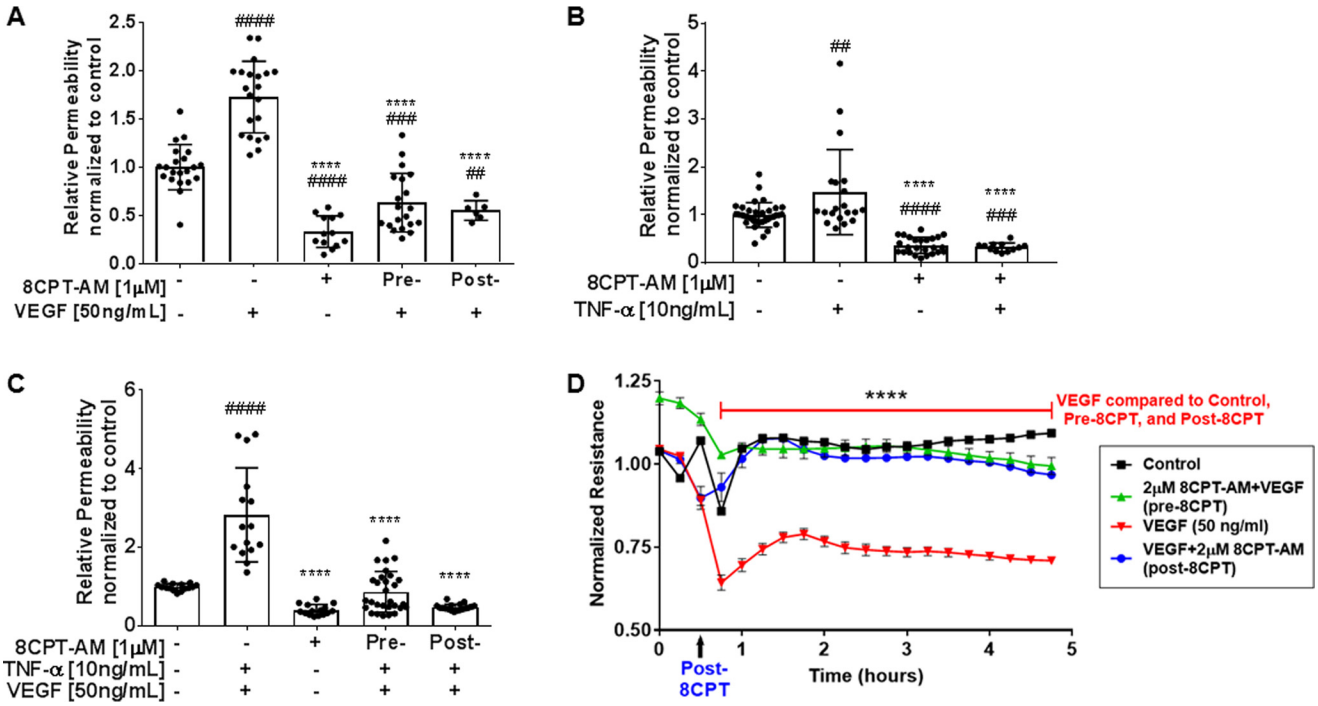


**Figure 3. 8-CPT-AM blocks and reverses permeability induced by VEGF and TNF-α.** *A*, BREC were stimulated with VEGF (50 ng/ml) or/and 8-CPT-AM (1 μM). *Pre*−, BREC were stimulated with 8-CPT-AM 30 min before VEGF treatment. *Post*−, BREC were treated with 8-CPT-AM 30 min after VEGF. 70 kDa RITC-dextran was added 30 min after the last treatment. Average $P_o$ values for control and VEGF were $9.7 \times 10^{-7}$ and $1.7 \times 10^{-6}$ (cm/s), respectively, $n \geq 6$. *B*, BREC were pretreated for 30 min before stimulated with TNF-α (10 ng/ml) and 70 kDa RITC-dextran was added 1 h later. Average $P_o$ values for control and TNF-α were $1.1 \times 10^{-6}$ and $1.7 \times 10^{-6}$ (cm/s), $n \geq 12$. *C*, BREC were stimulated with TNF-α (10 ng/ml) for 1 h followed by VEGF for 30 min. *Pre*−, 8-CPT-AM (1 μM) was added 30 min before TNF-α + VEGF or *Post*−, 8-CPT-AM (1 μM) was added 1.5 h after TNF-α + VEGF. 70-kDa RITC-dextran was added 30 min after the last treatment. Average $P_o$ values for control were $7.5 \times 10^{-7}$ and for TNF-α + VEGF were $1.9 \times 10^{-6}$ (cm/s), $n \geq 15$. Results are expressed as the mean relative to the control ± S.D. One-way analysis of variance: ##, $p < 0.005$; ###, $p < 0.001$; ####, $p < 0.0001$ compared with control. ****, $p < 0.0001$ compared with VEGF, TNF-α, or VEGF + TNF-α in *A*, *B*, and *C*, respectively. *D*, BREC were seeded on 8W10E+ arrays and TEER was measured every hour on the ECIS ZΘ instrument. 8-CPT-AM (2 μM) added 30 min prior to VEGF increases resistance and prevents VEGF-induced TEER loss for up to 6 h. 8-CPT-AM post-VEGF restores endothelial barrier after VEGF-induced ion permeability. Data represents the mean ± S.E. with analysis by two-way analysis of variance Bonferroni post hoc test: ****, $p < 0.0001$ compared with VEGF, $n = 3$/group.

in Rap1 activation (Fig. S2, *A* and *B*). Additionally, a VEGF time response was performed to determine whether VEGF directly affected active Rap1 levels in confluent BREC, but no differences in comparison to control were observed (Fig. S2, *C* and *D*).

Having established the ability of 8-CPT-AM to activate EPAC–Rap in BREC, we tested whether activation of EPAC increases endothelial barrier properties and reverses permeability after VEGF or TNF-α. A dose-response of 8-CPT-AM was performed in BREC both with and without VEGF, and permeability to 70-kDa rhodamine isothiocyanate (RITC)-dextran was measured. 8-CPT-AM at concentrations of 2, 1, and 0.5 μM significantly reduced basal permeability in comparison to control (Fig. 2*D*). To determine whether 8-CPT-AM was capable of blocking VEGF-induced retinal endothelial permeability, BREC were treated with varying doses of 8-CPT-AM for 30 min prior to VEGF (50 ng/ml) and solute flux was measured beginning 30 min after VEGF addition. 8-CPT-AM at concentrations of 2, 1, and 0.5 μM completely blocked VEGF-induced permeability (Fig. 2*E*). Based on these results, 1 μM 8-CPT-AM was used for all additional experiments unless otherwise stated.

To verify that 1 μM 8-CPT-AM was specifically activating the EPAC signaling pathway independently of PKA signaling, we quantified phosphorylation of CREB, a downstream PKA target. BREC were stimulated for 1 h with either 1 or 100 μM 8-CPT-AM, or with 100 μM forskolin (FSK) as a positive control to elevate cAMP (Fig. 2*F*). Cells were lysed and prepared for Western blot analysis. The BREC treated with FSK or 100 μM 8-CPT-AM had a 2-fold increase in phosphorylation of CREB, but 1 μM 8-CPT-AM did not increase phosphorylation of CREB (see Fig. 2, *F* and quantified in *G*).

To address the question of whether activation of the EPAC–Rap1 signaling pathway can reverse permeability, we pretreated BREC with VEGF or TNF-α followed by 8-CPT-AM and measured permeability to 70-kDa RITC-dextran using the solute flux assay. BREC were stimulated with cytokine (VEGF or TNF-α) alone, 8-CPT-AM alone, pretreatment with 8-CPT-AM 30 min prior to cytokine (pre-8-CPT), or treatment with cytokine 30 min prior to 8-CPT-AM treatment (post-8-CPT). The results demonstrate that 8-CPT-AM both prevents and reverses VEGF-induced endothelial permeability (Fig. 3*A*) or TNF-α–induced permeability (Fig. 3*B*). The combination of VEGF and TNF-α induces an additive 3-fold increase in endothelial permeability (Fig. 3*C*) and pretreatment with 8-CPT-AM completely prevents combined VEGF/TNF-α–induced permeability as well as reverses the effects of both VEGF/TNF-α (Fig. 3*C*).

Permeability to ions was also determined as a measure of paracellular permeability by measuring the transendothelial electrical resistance (TEER) in BREC monolayer using the ECIS

system. The BREC cells were either pretreated or post-treated with 8-CPT-AM (2 μM) and the monolayer's resistance was measured for 5 h. BREC treated with VEGF display a 40% decrease in TEER compared with control (Fig. 3*D*). BREC pretreated with 8-CPT-AM block VEGF from decreasing TEER, and BREC post-treated with 8-CPT-AM reverse the effects of VEGF and increase the TEER levels to control (Fig. 3*D*). To determine how long the 8-CPT-AM effect on VEGF reduction is maintained, we measured TEER for 24 h. 8-CPT-AM at 1 μM was statistically different from VEGF for 8 h (Fig. S3*A*), and a higher dose of 8-CPT-AM (5 μM) was statistically different from VEGF for 16 h (Fig. S3*B*).

### 8-CPT-AM prevents and reverses VEGF-induced tight junction disorganization

To assess the role of 8-CPT-AM in junctional complex organization we performed immunofluorescence staining of BREC TJs. Cells were treated with VEGF (50 ng/ml) for 1 h, 8-CPT-AM (1 μM) alone for 90 min, pretreated with 8-CPT-AM for 30 min followed by 1 h of VEGF, or treated with VEGF for 1 h prior to 30 min of 8-CPT-AM. VEGF induced significant disorganization, with large invaginations (*arrows*) and junctional border breaks (*arrowheads*) in all 3 TJ proteins analyzed (ZO-1, occludin, and claudin-5) (Fig. 4*A*) and as previously reported (30). 8-CPT-AM alone induced a significantly more linear and continuous organization of all 3 TJ proteins at the junctions in comparison to control as assessed by scoring in a blinded fashion (Fig. 4*A*). 8-CPT-AM pretreatment blocked and post-treatment reversed VEGF induction of TJ disorganization (Fig. 4*A*). It is notable that the increased cytoplasmic staining for both occludin and claudin-5 after VEGF treatment was not lost with 8-CPT-AM post-treatment but the border organization was dramatically increased. To determine whether 8-CPT-AM or VEGF was causing a change in total TJ protein levels, we performed Western blotting of the TJ proteins ZO-1, occludin, and claudin-5 after the same treatment with VEGF for 1 h, 8-CPT-AM for 90 min, or 8-CPT-AM + VEGF. TJ proteins ZO-1, occludin, and claudin-5 (Fig. 4, *B–E*) and adherens junction protein VE-cadherin (Fig. S4*A*) showed no total protein changes in this short time course, suggesting that EPAC–Rap1 activation promotes TJ assembly at the border.

### 8-CPT-AM attenuates VEGF signaling

The mechanistic connection between 8-CPT-AM and VEGF signaling was investigated by Western blotting for phosphorylation of signal transduction proteins known to function downstream of VEGF. BREC were treated with VEGF (50 ng/ml) for 15 min, 8-CPT-AM (1 μM) alone for 45 min, or pretreated with 8-CPT-AM for 30 min followed by VEGF for 15 min and compared with control cells. VEGF caused a significant increase in phosphorylation of VEGFR2 (Tyr-1175) and Erk1/2 (Fig. 5, *A–D*). 8-CPT-AM alone caused a 50% decrease in both Erk1 and Erk2 basal phosphorylation in comparison to control (Fig. 5, *C* and *D*). No phosphorylation changes were observed in VEGFR2 between control and 8-CPT-AM (Fig. 5*B*). However, pretreatment of 8-CPT-AM significantly reduced the phosphorylation of both VEGFR2 (Tyr-1175) and Erk1/2 in comparison to VEGF alone (Fig. 5, *B–D*). This effect was specific, as both VEGF and 8-CPT-AM promote an additive increase in AKT (Ser-473) phosphorylation (Fig. 5*E*).

### Inhibition of EPAC increases basal permeability in BREC

The EPAC inhibitor, HJC0350, was used in a dose-response solute flux assay. BREC were incubated with different HJC0350 concentrations for a total time of 45 min. HJC0350 at 5 and 10 μM caused approximately a 2-fold permeability increase (Fig. 6*A*). Inhibition of EPAC with HJC0350 at 5 and 10 μM blocked 8-CPT-AM (1 μM) from decreasing basal permeability. To determine potential cytotoxicity of HJC0350, a viability assay was performed. Viability of BREC treated with HJC0350, ESI 09 (an inhibitor of both EPAC1 and EPAC2), DMSO (50% as a positive control for BREC cytotoxicity), and VEGF (50 ng/ml) were tested for 1.5 h using the CellTiter-Fluor Cell Viability assay. VEGF, HJC0350 (0.1–50 μM), and ESI 09 (1–10 μM) did not cause cell death (Fig. S5), whereas 50% DMSO caused ~75% cell death, and 30 μM ESI 09 caused 33% cell death (Fig. S5).

To determine which EPAC isoform contributes to regulating basal permeability properties we used siRNA to knock down EPAC1 or EPAC2 specifically and measured solute flux. BREC with EPAC1 knockdown demonstrated a 3-fold permeability increase in comparison to control siRNA (Fig. 6*B*). EPAC2 knockdown did not show a difference in basal permeability in comparison to control BREC. Additionally, we performed a double knockdown of EPAC1 and -2 and observed a 3.5-fold increase in permeability in comparison to control (Fig. 6*C*), similar to EPAC1 knockdown alone. Fig. 6, *D* and *E*, reveal siRNA to EPAC1 yielded a 58% knockdown and siRNA to EPAC2 yielded a 65% knockdown as measured by qRT-PCR. In all knockdown conditions, 8-CPT-AM could still induce barrier properties likely due to incomplete knockdown of EPAC. Collectively, these data reveal EPAC1 contributes to basal barrier properties in BREC.

### Rap1B isoform regulates basal permeability and tight junction organization

Mammals possess two isoforms of EPAC proteins, EPAC1 and EPAC2, and two isoforms of Rap1 proteins, Rap1A and Rap1B (17, 31). We designed primers for each isoform and performed PCR demonstrating BREC express mRNA for both Rap1A and Rap1B isoforms, as well as EPAC1 and EPAC2 isoforms (Fig. 7*A*). A composite of 3 Rap1A and 3 Rap1B specific siRNAs (transfected at 100 nM) caused a specific Rap1A or Rap1B knockdown, respectively, in BREC as measured by qRT-PCR (Fig. 7*B*). Furthermore, Rap1B siRNA caused a 66% knockdown of Rap1 protein in BREC as assessed by Western blot analysis (Fig. 7*C*), whereas Rap1A siRNA had no effect (Fig. S6*A*). This antibody detects both Rap1A and -B, and no isoform-specific antibody is available. To determine the role of Rap1B in basal endothelial permeability, we silenced the *Rap1B* gene in BREC and measured permeability using the 70-kDa solute flux assay. BREC with scramble siRNA behaved comparably to wild-type BREC in response to both VEGF and 8-CPT-AM (Fig. 7*D*). BREC with Rap1B knockdown demonstrated a 2-fold increase in basal permeability comparable with

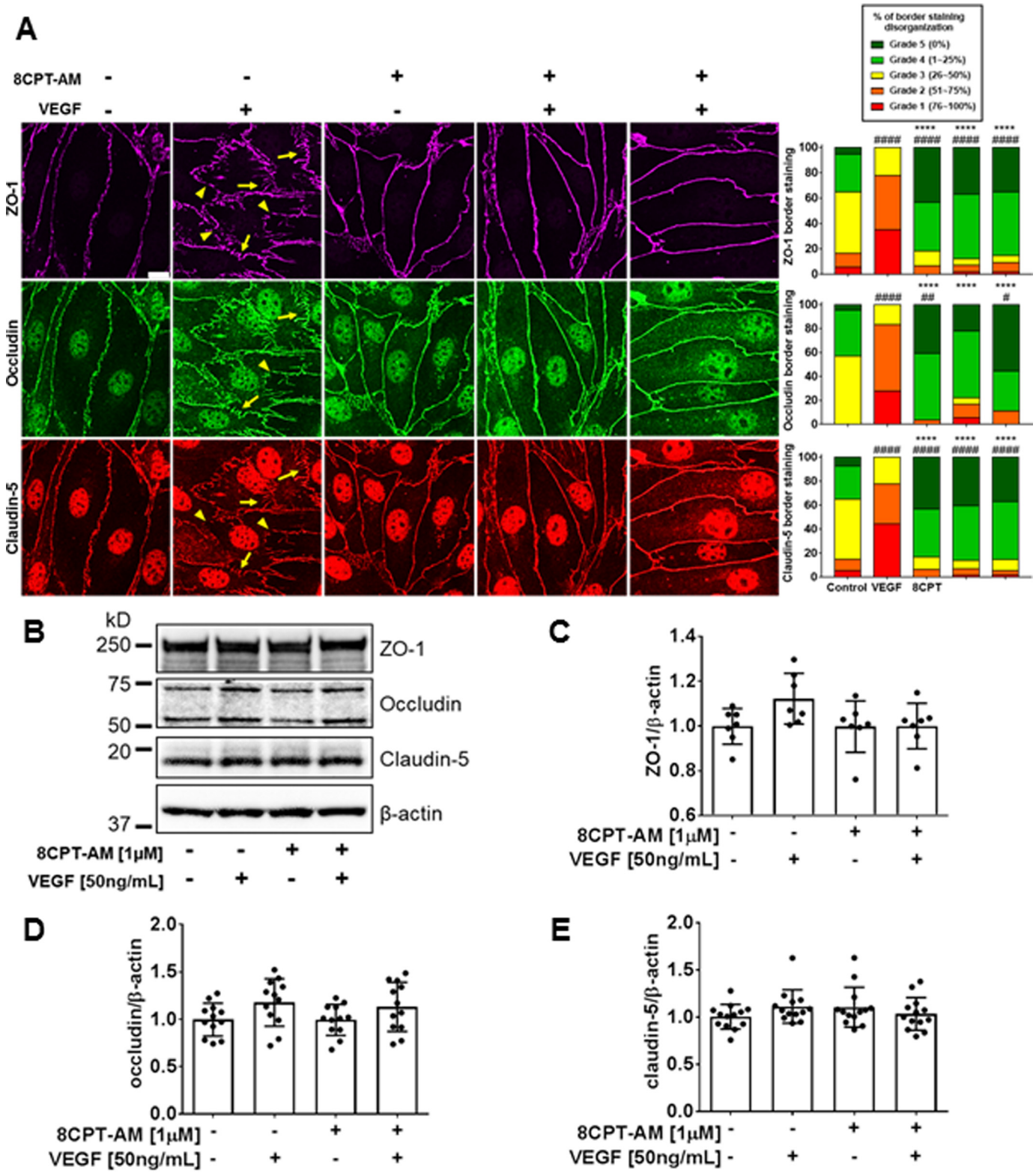


**Figure 4. 8-CPT-AM prevents and reverses VEGF-induced tight junction disorganization.** *A,* immunofluorescence staining of TJ proteins ZO-1, occludin, and claudin-5 was performed to assess their organization after the addition of 8-CPT-AM (1 $\mu$M) for 30 min and/or VEGF (50 ng/ml) for 1 h. *Yellow arrows* show loss of linear organization (invaginations), and *yellow arrowheads* show border breaks or gaps between adjacent cells. Histograms show scoring of TJ proteins as percent organization. ZO-1, occluding, and claudin-5 border staining were quantified by a semi-quantitative ranking score system based on a graded scale from 1 to 5: *Grade 1* for near complete disorganization of border staining 0 to 25%; *Grade 2* for 25 to 50% continuous border staining; *Grade 3* for 50 to 75% continuous border staining; *Grade 4* for 75% to 100% continuous border; and *Grade 5* completely continuous border. *B,* changes in TJ total protein expression with VEGF or 8-CPT-AM were measured using Western blot analysis. *C–E,* no changes in ZO-1, occludin, and claudin-5 expression were observed in any of the experimental conditions. Results are expressed as the mean relative to the control ± S.D. with analysis by one-way analysis of variance and Bonferroni post hoc test: #, $p < 0.01$; ##, $p < 0.005$; ####, $p < 0.0001$, or ****, compared with VEGF.

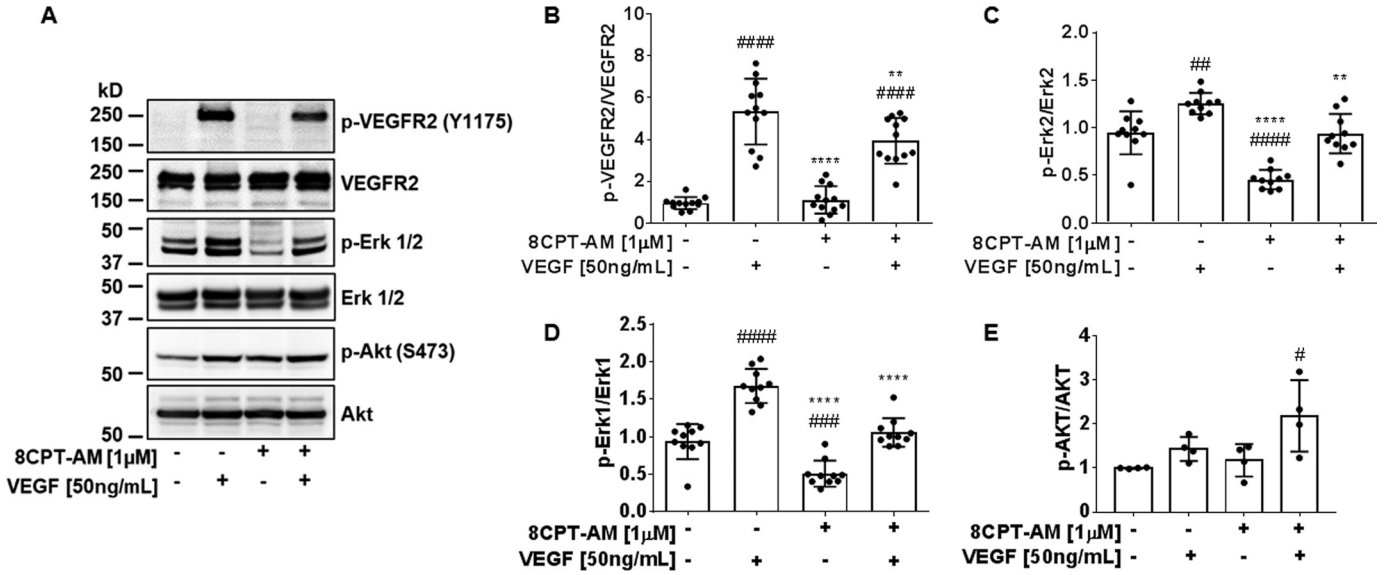


**Figure 5. 8-CPT-AM attenuates VEGF-Erk1/2 signal transduction.** *A,* immunoblotting was used to detect phospho-Tyr-1175 and total VEGFR2, phospho and total Erk1/2, and phospho-Ser-473 and total AKT changes in BREC pre-treated with 8-CPT-AM (1 $\mu$M) for 30 min followed by 15 min of VEGF (50 ng/ml). *B,* VEGFR2 Tyr-1175 phosphorylation was reduced by 8-CPT-AM when added prior to VEGF, $n \geq 12$. *C,* 8-CPT-AM decreased Erk1 and *D,* Erk2 phosphorylation, $n \geq 10$. *E,* both VEGF and 8-CPT-AM increase AKT phosphorylation, $n \geq 4$. Values are mean ± S.D. ####, $p < 0.0001$ or ###, $p < 0.001$ or ##, $p < 0.005$ or #, $p < 0.05$ compared with control and ****, $p < 0.0001$ or **, $p < 0.01$ compared with VEGF.

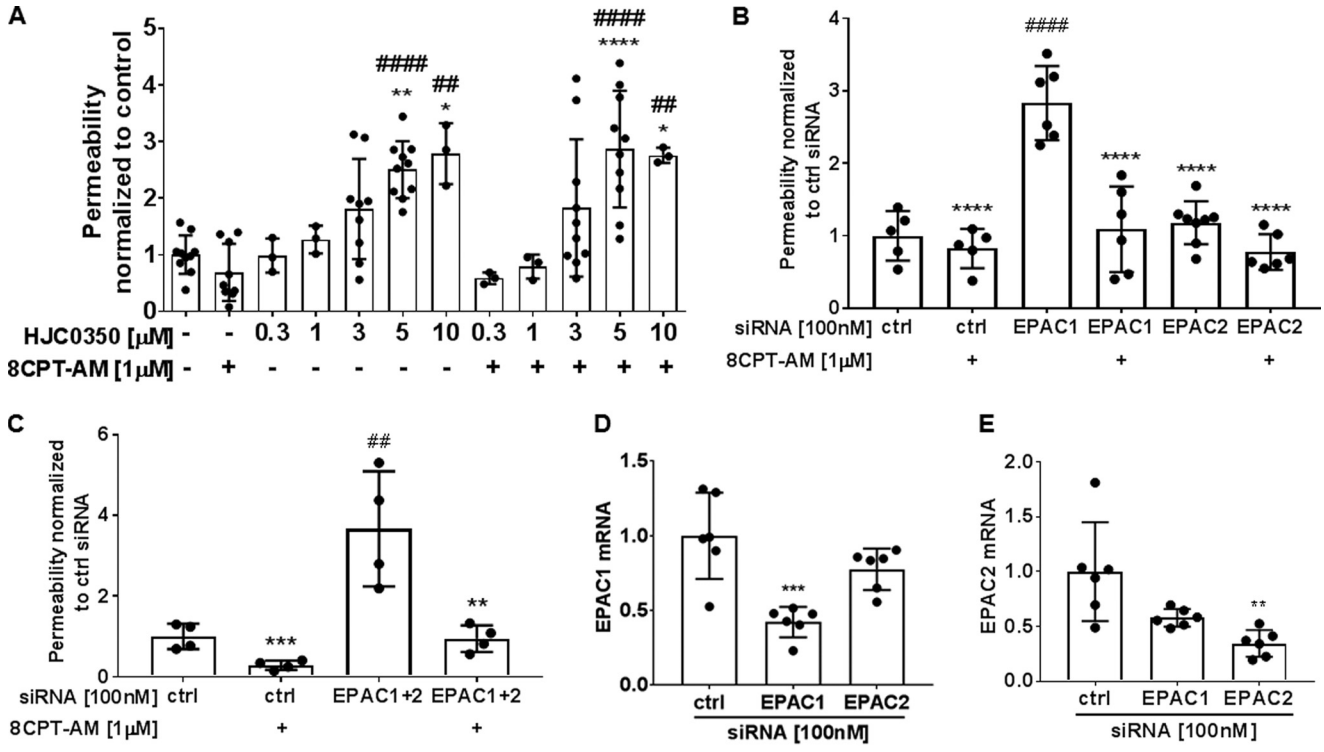


**Figure 6. EPAC contributes to basal barrier properties in BREC.** *A,* solute flux assay was used to test EPAC antagonist, HJC0350, at different concentrations on BREC. HJC0350 5 to 10 $\mu$M had a significant increase in basal permeability and blocked 8-CPT-AM barrier induction. Average $P_o$ values for control and HJC0350 were $2.2 \times 10^{-7}$ and $4.4 \times 10^{-7}$ (cm/s). Results are expressed as the mean ± S.D. relative to the control with a total of $n \geq 3$, ####, $p < 0.0001$ or ##, $p < 0.001$ compared with control or scramble control in *B* and *C* and ****, $p < 0.0001$; ***, $p < 0.001$; **, $p < 0.01$; *, $p < 0.05$ compared with 8-CPT-AM or siRNA EPAC1 in *B* or siRNA EPAC1 and EPAC2 in *C*. *B,* solute flux assay was used to test permeability in BREC with either EPAC1 or EPAC2 knockdown. Scramble (*ctrl*), EPAC1 and EPAC2 siRNA at 100 nM were used in BREC. Average $P_o$ values for scramble control, EPAC1 and EPAC2 siRNA were $1.1 \times 10^{-7}$, $3.1 \times 10^{-7}$, and $1.3 \times 10^{-7}$ (cm/s). *C,* solute flux assay was used to test permeability in BREC with double knockdown of EPAC1 and EPAC2 in BREC. EPAC1 and EPAC2 siRNA were used at 100 nM. Average $P_o$ values for scramble control and double EPAC1 and 2 siRNA were $0.86 \times 10^{-6}$ and $3.1 \times 10^{-6}$ (cm/s). *D,* SYBR Green qRT-PCR was used to quantify EPAC1 and *E,* EPAC2 mRNA after siRNA knockdown.

VEGF treatment (Fig. 7*D*); notably this response was also comparable with addition of the EPAC antagonist or EPAC1 siRNA (Fig. 6). VEGF addition to BREC with Rap1B knockdown had no additional change in permeability. BREC with Rap1B knockdown had a significant decrease in basal permeability in the presence of 8-CPT-AM, which could be due to the presence of

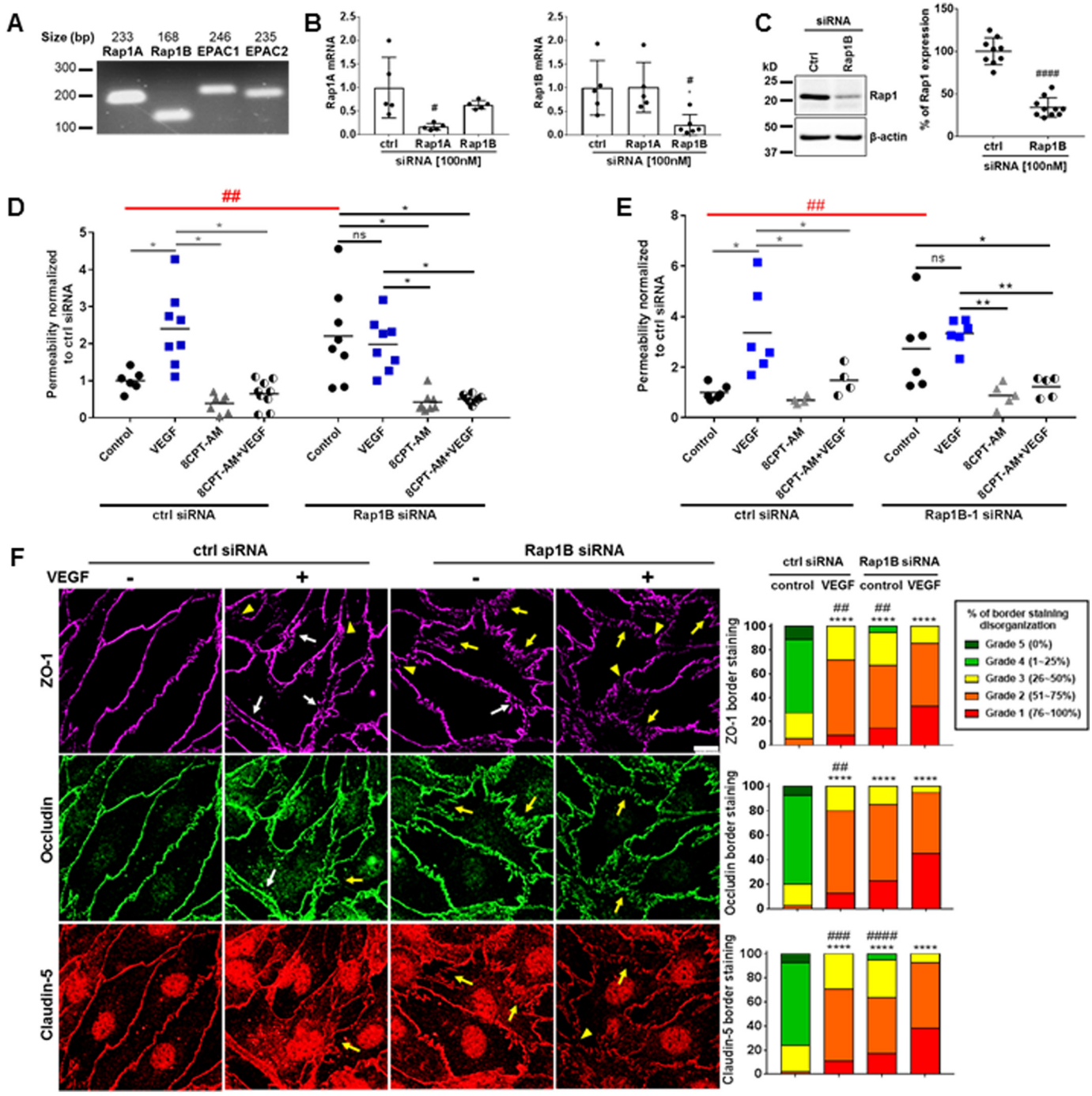


**Figure 7. Rap1B contributes to basal permeability and tight junction organization.** *A,* both Rap1 (Rap1A and Rap1B) and EPAC (EPAC1 and EPAC2) isoforms were found to be present in BREC by PCR. *B,* SYBR Green qRT-PCR was used to test Rap1 isoform siRNAs specificity. #, $p < 0.05$. *C,* Western blot shows that composite Rap1B (100 nM) siRNA results in a 66% knockdown, Student's *t* test ####, $p < 0.0001$, $n \geq 9$. *D,* solute flux assay was used to test permeability in BREC with Rap1B knockdown. Scramble and Rap1B siRNA at 100 nM were used in BREC. Average $P_o$ values for scramble control and Rap1B siRNA control were $2.4 \times 10^{-7}$ and $5.4 \times 10^{-7}$ (cm/s). *E,* solute flux assay was used to test permeability in BREC with individual Rap1B-1 siRNA. Scramble and Rap1B-1 siRNA at 100 nM were used in BREC. Average $P_o$ values for scramble control and Rap1B-1 siRNA control were $9.0 \times 10^{-8}$ and $2.3 \times 10^{-7}$ (cm/s). *F,* immunofluorescence staining of TJ proteins ZO-1, occludin, and claudin-5 was performed to assess the organization of TJ proteins after Rap1B knockdown with and without VEGF (50 ng/ml) for 1 h. *Scale bar,* 10 $\mu$m. Histograms of scoring TJ show % organization of TJs. All results are expressed as the mean relative to the scramble control with a total of $n > 4$. ZO-1, occludin, and claudin-5 border staining were assessed by semi-quantitative ranking score system based on scale grades from 1 to 5. Immunofluorescence results are expressed as the mean relative to the scramble control $n \geq 4$ with analysis by one-way analysis of variance and Bonferroni post hoc test, ****, $p < 0.0001$ compared with scramble control and ##, $p < 0.05$; ###, $p < 0.001$; ####, $p < 0.0001$ compared with Rap1B siRNA VEGF. Permeability results are expressed as the mean relative to the scramble control two-way analysis of variance analysis and Bonferroni post hoc test: *, $p < 0.05$; **, $p < 0.01$; and ##, $p < 0.01$ comparison between scramble and Rap1B or Rap1B-1 siRNA controls.

Rap1A or Rap2 isoforms or failure of complete Rap1B knockdown (Fig. 7*D*). To ensure specificity of the composite Rap1B siRNA, the 3 siRNAs were tested individually and one of the siRNAs (Rap1B-1 siRNA) was found to yield a 58% knockdown of Rap1 expression (Fig. S6*B*) comparable with the composite Rap1B siRNA. Rap1B-1 siRNA at 100 nM again led to a signifi-

cant increase in basal permeability in comparison to scramble siRNA control (Fig. 7*E*).

To determine whether *Rap1B* contributes to TJ organization, we silenced Rap1B expression in BREC using siRNA followed by immunofluorescence staining of the TJ proteins ZO-1, occludin, and claudin-5. Scramble siRNA had no effect on basal organization, and BREC treated with VEGF for 1 h showed disorganization of all three TJ proteins (Fig. 7*F*). BREC with Rap1B knockdown showed a significant percentage of TJ disorganization in comparison to scramble siRNA control with invaginations (*arrows*), gaps (*arrowheads*), and regions of border separation between cells (*white arrows*) (Fig. 7*F*). The combination of VEGF and Rap1B knockdown showed an even greater effect on TJ disorganization in comparison to scramble siRNA with VEGF. Similar to the solute flux assay results, BREC with Rap1B knockdown treated with 8-CPT-AM alone or with 8-CPT-AM plus VEGF for 1 h showed increased organization of the TJs at the cell border (Fig. S6*C*). These results are likely due to the remaining Rap protein available to respond to 8-CPT-AM.

## Discussion

The present study provides compelling evidence that activation of the EPAC–Rap1 signaling pathway via the cAMP analog, 8-CPT-AM, promotes barrier properties in retinal vascular endothelial cells. Previous research on the role of EPAC–Rap1 signaling in barrier properties has focused on HUVEC and epithelial cells (32, 33). In this work, we demonstrate that the GEF, EPAC, and the small GTPase, Rap1B, regulate basal retinal endothelial barrier properties and contribute to TJ complex organization. We demonstrate that activation of EPAC–Rap1 blocks permeability induced by VEGF and TNF-$\alpha$ both in cells and *in vivo*. Importantly, activation of EPAC–Rap1 reverses permeability induced by these cytokines in cell culture and reverses retinal vascular permeability induced by ischemia reperfusion *in vivo*. 8-CPT-AM activation of EPAC–Rap1 regulates TJ organization and reverses the effect of TJ disorganization by VEGF, which likely contributes to the control of endothelial barrier properties. We further show that 8-CPT-AM specifically attenuates the VEGF–ERK signaling pathway. Together these data indicate that EPAC–Rap1 signaling contributes to basal barrier properties and TJ organization of retinal endothelial cells and activating this pathway can restore barrier properties of the BRB.

Previous studies support a role for activation of the EPAC–Rap1 signaling pathway in blocking permeability induced by permeabilizing agents. *In vivo* studies show that activation of the EPAC–Rap1 signaling pathway attenuates platelet-activating factor-induced permeability in the mesenteric microvasculature (26) and inhibits VEGF-induced dermis vascular permeability (22). Activation of the EPAC–Rap1 signaling pathway also has been shown to block thrombin-induced permeability in HUVEC (24). Additionally, activation of the EPAC–Rap1 pathway restores barrier properties in endothelial cells and in blood vessels. For example, activation of EPAC–Rap1 reverses the TEER decrease caused by TNF-$\alpha$ and TGF-$\beta$ in HUVEC (34). Our study builds upon these previous reports demonstrating that activation of EPAC–Rap1 reversed IR-induced permeability *in vivo* and reversed VEGF- and TNF-$\alpha$–induced permeability in BREC and *in vivo*. Together these data show pharmacologic activation of EPAC–Rap1 signaling promotes and restores the BRB.

The EPAC1 and EPAC2 protein isoforms are both expressed in the retina (35). In the endothelium, EPAC1, but not EPAC2, is expressed in HUVEC (25). EPAC2 has been detected in human pulmonary aortic endothelial cells (24), and we show that EPAC1 and -2 mRNA are present in BREC. EPAC1 is known for its involvement in regulating cell-cell junctions and endothelial barrier properties (25, 32), and EPAC2 has been observed in modulating neuronal activity (36). Here, we show that EPAC1 plays a role in retinal endothelial barrier. In BREC, when EPAC is pharmacologically inhibited, basal permeability is increased, and 8-CPT-AM cannot restore the barrier. Using siRNA specific for EPAC1 and -2 reveals a role for EPAC1 in basal permeability in BREC. In a previous study, it was observed that ischemic retinopathy in EPAC2-deficient mice induced a more severe retinal edema and a larger expression of aquaporin AQP4 surrounding the blood vessels in the inner BRB in comparison to the EPAC1-deficient mice (37). The EPAC2- and EPAC1-decificient mice, without ischemic retinopathy, appeared relatively normal in comparison to the wild-type mice. Future studies may address the role of EPAC in BRB properties after cytokine challenge or diabetes.

The Rap1B isoform contributes a major role in endothelial barrier regulation, vasculogenesis, and angiogenesis (19, 38). Even though the Rap1 isoform proteins have a high protein sequence homology, gene deletion studies on mice of the individual *Rap1* isoforms show different viability outcomes. The *Rap1A* null mice were viable and had no size difference in comparison to wild-type mice. On the other hand, the *Rap1B* null mice show an 80% embryonic lethality between embryonic (E) days 13.5 and 18.5 (39, 40). Global or endothelial specific double *Rap1A* and *Rap1B* gene deletion is completely embryonic lethal and mice die within E10.5 to E15.5 (19). Post-mortem analysis revealed that *Rap1B* and double *Rap1A* and *Rap1B* null mice manifested vascular hemorrhage (19, 20). The *Rap1B* null viable mice exhibited defective angiogenesis, which led to a retardation in retinal neovascularization (20). Consistent with these studies, we reveal that silencing the *Rap1B* gene in BREC was sufficient to induce an increase in endothelial permeability and disruption of the TJs. However, addition of 8-CPT-AM decreased solute flux and promoted TJ organization at the cell periphery in BREC with Rap1B knockdown. These data are unsurprising Rap1A as well as Rap2A/B/C, or residual Rap1B from incomplete knockdown, may compensate with the pharmacologic dose of 8-CPT-AM and EPAC activation.

Activation of the EPAC–Rap1 pathway contributes to endothelium barrier properties through junction complex maintenance (41) and down-regulation of small G-protein RhoA, known to be involved in permeability (42). EPAC activation in HUVEC leads to the recruitment of VE-cadherin to the cell border and formation of long linear and continuous adherens junctions (24). VE-cadherin-mediated junctional organization in HUVEC results in a decrease in solute flux (25). Additional observations of EPAC–Rap1 activation include reduction of actin stress fiber formation, and maintenance of VE-cadherin

and cortical actin at the cell periphery (24). Here, we show for the first time in BREC that EPAC–Rap1 signaling protects TJ organization of the proteins ZO-1, occludin, and claudin-5. EPAC–Rap1 signaling blocks and reverses VEGF-induced TJ invaginations, gap formations, and TJ border breaks. As it has been observed with VE-cadherin organization (24, 25), we also observed that 8-CPT-AM alone increases the recruitment and continuous linear organization of TJ at the cell border but does not increase TJ protein expression.

The mechanism by which activation of EPAC–Rap1 recruits and maintains TJ proteins at the cell borders of BREC remains to be fully understood. However, studies in endothelial cells show that organization and stabilization of the adherens junctional complex proteins may occur through the recruitment and interaction of afadin (AF-6) and Krev interaction trapped 1 (Krit1) with active Rap1 (43, 44). In human pulmonary artery endothelial cells, activation of Rap1 promotes colocalization of AF-6 with both VE-cadherin and ZO-1 and interaction between AF-6 and p120-catenin (44). In HUVEC active Rap1 recruits Krit1 to the cell-cell junctions, which interacts with $\beta$-catenin, p120-catenin, and AF-6 but not with ZO-1 (43). Therefore, additional studies are necessary to determine whether EPAC–Rap1 activation mediates TJ recruitment and organization in BREC via AF-6.

Permeabilizing agents such as VEGF, TNF-$\alpha$, and thrombin all activate RhoA (24, 44, 45). Activation of RhoA induces stress fiber formations associated with junctional complex alterations and formation of intercellular gaps resulting in increased permeability (46). Inhibition of RhoA downstream targets such as RhoA/Rho kinase (ROCK) blocks permeability (45). In HUVEC, activation of EPAC–Rap1 signaling reduced permeability induced by permeabilizing agents by down-regulating RhoA activity (24). Studies in HUVEC show that active Rap1 interacts with rasip1 and together with Rap associating with the DIL domain (radil), recruits Rho GTPase-activating protein 29 (ArhGAP29), which down-regulates RhoA activity (47). Recently, it has been observed that rasip1 and radil are recruited to the cell membrane via the transmembrane protein heart of glass 1 (HEG1) (48). An interesting finding from this group showed that interaction of Rap1–rasip1 and rasip1—radil–ArhGAP29 was not affected by HEG1 knockdown. Immunofluorescent studies show that rasip1 has a perinuclear localization (49) but moves to the cell border during nascent junction formation after a calcium switch assay (50). Together these data suggest that rasip1 serves a dual function, to interact with radil and ArhGAP29 to suppress RhoA activity and localizing to the cell border through HEG1 where it regulates recruitment and stabilization of junctional proteins, for a mechanism schematic refer to Ref. 51.

Studies of the outer retina show that Rap1 activation promotes barrier integrity in the RPE and inhibits choroidal neovascularization (28, 52). In a retinal epithelial cell line (ARPE-19) Rap1 knockdown led to mislocalization of cadherins and a decrease in transepithelial electrical resistance (52) in a Rap1A-specific manner (28). Studies in RPE show that Rap1A regulates barrier integrity by modulating the interaction of $\beta$-catenin and IQGAP, a scaffold protein involved in actin cytoskeleton and cell-cell adhesion regulation (53, 54). This barrier stabilization inhibits choroidal endothelial cells transmigration (28, 55). The results from the ARPE-19 cells and *in vivo* studies indicate that the Rap1A isoform is the major contributor to RPE barrier integrity in contrast to the role of Rap1B in retinal vascular endothelial barrier properties observed here. These data suggest that individual Rap1 isoforms control barrier properties in a cell-specific manner.

Rap1 signaling regulates several cell processes including suppression of the Ras–Raf–Erk signaling pathway (56). The extracellular signal-regulated kinase (Erk1/2) is involved in several cell pathways including but not limited to cell proliferation, cell survival, and migration (57). In retinal endothelial cells, binding of VEGF to the VEGFR2 induces an increase in Erk1/2 signaling. We showed that in BREC, activation of EPAC–Rap1 signaling attenuates the Erk1/2 signaling and reduces the phosphorylation of the VEGFR2 on Tyr-1175. Previous studies have shown VEGFR2 activation leads to activation of the kinase, PKC$\beta$, which phosphorylates occludin, promoting ubiquitination and leading to endocytosis of occludin and other junctional proteins, resulting in permeability (27, 58, 59). Even though 8-CPT-AM addition blocks VEGF-induced permeability, 8-CPT-AM does not attenuate phosphorylation of (Ser-490) occludin (data not shown). 8-CPT-AM treatment does reverse or prevent the internalization of junctional proteins suggesting either dominance of the junctional assembly pathway or inhibition of junctional internalization at a separate step.

In conclusion, the EPAC -Rap1 pathway, specifically the EPAC1 and Rap1B isoforms, contributes to basal permeability. Further, stimulating the EPAC-Rap pathway shows promise as a therapeutic strategy to restore barrier properties after VEGF or inflammatory cytokine-induced permeability.

## Experimental procedures

### *Reagents*

The following reagents were purchased from Tocris Bioscience: the cAMP analog 8-CPT-AM specific for EPAC (catalogue number 4853), EPAC2 inhibitor (HJC 0350) 2,4-dimethyl-1-[(2,4,6-trimethylphenyl) sulfonyl]-1H-pyrrole (catalogue number 4844), and EPAC inhibitor (ESI 09) $\alpha$-[(2-(3-chlorophenyl)hydrazinylidene]-5-(1,1-dimethylethyl)-$\beta$-oxo-3-isoxazolepropanenitrile (catalogue number 4773). Recombinant human VEGF165 was from R&D Systems (Minneapolis, MN). Power SYBR Green PCR Master Mix (catalogue number 4367659) was from Thermo Fisher Scientific (Warrington, UK).

### *Antibodies*

The following antibodies were used for Western blotting. Purchased from Cell Signaling were: AKT rabbit polyclonal (pAb) (catalogue number 9272), phospho-AKT (Ser-473) rabbit monoclonal (mAb) (catalogue number 4060), phospho-CREB (Ser-133) rabbit mAb (catalogue number 9198), CREB rabbit mAb (catalogue number 9197), VEGFR2 rabbit mAb (catalogue number 2479), phospho-VEGFR2 (Tyr-1175) rabbit mAb (catalogue number 3770), Erk1/2 rabbit pAb (catalogue number 9102), phospho-Erk1/2 (T202/Y204) mouse (catalogue number 9106L), and $\beta$-actin mouse mAb (catalogue number 3700). EPAC rabbit pAb (catalogue number sc-25632) was pur-

chased from Santa Cruz Biotechnology (Santa Cruz, CA). The following were used in tissue and cell staining: Rap1A mouse mAb (catalogue number sc-373968) Santa Cruz Biotechnology; IB4, Hoescht); ZO-1 rat (catalogue number MABT11, Millipore), Claudin-5 rabbit (catalogue number 34-1600, Invitrogen), and Occludin mouse 488 Alexa (catalogue number 331588, Lifetech, USA).

### *In vivo permeability assays*

For the Evan's Blue permeability assay, male Long-Evans rats (Charles River Laboratories, Wilmington, MA) weighing 200–250 g were housed in accordance with the guidelines of the institutional animal care and use committee (IACUC) and consistent with the ARVO Statement for the Use of Animals in Ophthalmic and Visual Research. The IACUC approved all animal procedures. Rats were anesthetized with intramuscular injection of ketamine and xylazine (66.7 and 6.7 mg/kg of body weight, respectively). A 32-gauge needle was used to create a hole for an intravitreal injection (2 $\mu$l/eye) using a 5-$\mu$l Hamilton syringe. The experimental animal groups received an intravitreal injection of VEGF (50 ng) and TNF-$\alpha$ (10 ng) together, or VEGF/TNF-$\alpha$/8-CPT-AM either at 10 (355 ng) or 50 $\mu$M (1.78 $\mu$g) simultaneously. The animals recovered for 3 h and were then anesthetized again for the permeability assay as described by our group previously (60).

### *Ischemia reperfusion assay*

For studies using ischemia reperfusion to induce vascular permeability and retinal sterile inflammatory response, mice were anesthetized with ketamine and xylazine. Mice underwent ischemia on their left eye by inserting a needle horizontally into the anterior chamber of the eye and avoiding the lens. The intraocular pressure in the anterior chamber is increased to 120 mm Hg with PBS and maintained constant for 90 min to block the blood supply from the retinal artery followed by natural reperfusion, as described previously (27).

### *Solute flux assay*

Primary BREC were isolated and grown in culture as previously described (61) to model the vascular endothelial blood-retinal barrier *in vitro* (30). BREC were seeded on 0.4-$\mu$m pore transwells filters (Corning Costar, Acton, MA) coated with 1 $\mu$g/cm$^2$ fibronectin. BREC were grown to confluence in MCDB-131 medium, supplemented with 10% fetal bovine serum (FBS), 22.5 $\mu$g/ml of endothelial cell growth factor, 120 $\mu$g/ml of heparin, 0.01 ml/ml of antibiotic/antimycotic. Then cell culture media was changed to stepdown media, MCDB-131 supplemented with 1% FBS, 0.01 ml/ml of antibiotic/antimycotic, and 100 nmol/liter of hydrocortisone, for 48 h prior to the experiment. For experiments with TNF-$\alpha$ treatment, no hydrocortisone was in the stepdown media. The cells were treated with VEGF (50 ng/ml) for 30 min, and/or with TNF-$\alpha$ (10 ng/ml) or 8-CPT-AM (1 $\mu$M unless otherwise stated) for the indicated time. Cell monolayer permeability to 70-kDa RITC-dextran (Sigma) was calculated by measuring the rate of flux of the substrate over a 4-h time course followed by calculating the diffusive permeability ($P_o$) across the monolayer (62).

$$P_o = [(F_L/\Delta t)V_L]/(F_A A) \quad \text{(Eq. 1)}$$

Where $P_o$ is in cm/s, $F_L$ is basolateral fluorescence, $F_A$ is apical fluorescence, $\Delta t$ is the change in time, $A$ is the surface area of the filter, and $V_L$ is the volume of the basolateral chamber.

### *TEER assay*

Cell monolayer ion flux was measured by electrical resistance using an electrical cell-substrate impedance sensing (ECIS)-ZΘ system at 4000 Hz (Applied Biophysics, Troy, NY). BRECs were seeded on 8-well 8W10E$^+$ ECIS plates containing gold electrodes. Cells were left to grow overnight or until 90% confluent followed by media changed to stepdown media for 48 h. After 48 h of stepdown the monolayers of cells were treated with compounds of interest.

### *GTP bound Rap1 pulldown and detection assay*

Pulldown for active Rap1 based on capture using the GST-linked peptide of the downstream Rap1 effector Ral guanine nucleotide dissociation stimulator (RalGDS) Rho-binding domain (RBD) kit was purchased from (Thermo Scientific, Rockford, IL) (kit catalogue number 16120) and used per the manufacturer's instructions. Cells were lysed with 500 $\mu$l of 1× lysis/binding/wash buffer provided in the kit, centrifuged at 16,000 × *g* for 15 min at 4 °C, and the supernatant was transferred onto a spin cup collection tube containing glutathione resin. GST–RalGDS–RBD fusion protein (20 $\mu$g/spin cup) was added to the supernatant and incubated for 1 h with gentle rocking at 4 °C. Samples were then centrifuged at 6,000 × *g* for 30 s, washed 3 times, and eluted with 50 $\mu$l of 2× reducing sample buffer (1-part $\beta$-mercaptoethanol to 20 parts 2× SDS sample buffer; Thermo Scientific). Eluted samples, 25 $\mu$l, and total cell lysates, 30 $\mu$g, were loaded onto NuPAGE SDS gels for Western blot analysis. Captured GTP-bound Rap1, as well as total Rap1 protein in lysate was detected using the anti-Rap1 rabbit mAb provided by the GTP-Rap1 pull-down kit (Thermo Scientific).

### *Immunofluorescent staining*

For immunofluorescent staining and imaging, BREC were fixed with 1% paraformaldehyde for 10 min at room temperature. The cells were permeabilized with 0.2% Triton X-100 followed by blocking with 10% milk in 0.1% Triton X-100 for 1 h at room temperature. Cells were stained with primary antibodies for 2 days at 4 °C. Cells were washed, then stained with secondary antibodies overnight at 4 °C. Cells were imaged with Leica confocal microscope (TCS SP5; Wetzlar, Germany).

### *Western blot*

Cell lysates, 30 $\mu$g of protein, were loaded into each well of NuPAGE SDS gels (Life Technologies) and separated by electrophoresis. After nitrocellulose membrane transfer, membranes were blocked in 2% ECL Prime Blocking Reagent and incubated with primary antibodies overnight at 4 °C. Secondary antibodies IgG conjugated with HRP were detected with Lumigen ECL ultra chemiluminescent reagent (TMA-100, Lumigen, Inc., Southfield, MI).

### *Viability assay*

To measure viability of cells, the CellTiter-Fluor Cell Viability assay was used according to the manufacturer's protocol

(Promega, Madison, WI). The fluorescent signal proportional to the number of living cells is generated by the cell-permeant peptide substrate (glycyl-phenylalanyl-aminofluorocoumarin), which is cleaved by live cell protease activity. Cells were grown on a 96-well plate until they reached confluence and then changed to step down media for 48 h. VEGF (50 ng/ml), DMSO (50%), ESI 09, HJC 0350, or vehicle were diluted in media, applied to the cells at a final volume of 100 $\mu$l, and incubated for 1 h. The CellTiter-Fluor Reagent was added in an equal volume, mixed briefly using an orbital shaker, and incubated for 30 min at 37 °C. Fluorescence was measured after 1.5 h using a fluorometer (excitation 355 nm/emission 520 nm).

### Gene expression knockdown experiments

Composite and individual Rap1B siRNAs specific for bovine (sc-270595, sc-270595A (Rap1B-1 siRNA), sc-270595B, and sc-270595C; Santa Cruz Biotechnology) and composite bovine-specific EPAC1 and EPAC2 siRNAs (sc-270604 and sc-270605) were purchased from Santa Cruz Biotechnology. BRECs were transiently transfected with 100 nM of either experimental gene siRNA or scramble (ctrl) siRNA (siGENOME Non-Targeting siRNA#1, D-001210-01-05; Dharmacon GE Healthcare) using the nucleofection technique (Lonza). Briefly, cells were trypsinized and $5 \times 10^5$ cells were used per nucleofection. Nucleofection solution and supplement solution were used to resuspend the cell pellet in a final volume of 100 $\mu$l. The cell suspension was mixed with 100 nM siRNAs in cuvette and nucleofection was carried out per the manufacturer's instructions (setting S-05; Amaxa Biosystems). Cell were diluted with 0.5 ml of MCDB-131 media and added onto 6-well plates containing 1.5 ml of media. Nucleofected cells were gently mixed in a total of 2 ml of media, then 0.5 ml of cell suspension was plated directly onto fibronectin-coated 0.4-$\mu$m pore transwell filters. After 4 h, the media was replaced with fresh MCDB-131 media. Confluent cells were then changed to step down media for 48 h and treated with compounds of interest followed by *in vitro* Solute Flux assay as described above.

### qRT-PCR

Total RNA was isolated from BREC after gene expression knockdown using the RNeasy Plus Mini kit (catalogue number 74134 from Qiagen). Complementary DNA (cDNA) was synthesized using oligo(dT) primers and the OmniScript reverse transcriptase (Qiagen). For the qRT-PCR the specific oligonucleotide primers used, forward and reverse, respectively, were as follows: for Rap1A, 5′-GCCAACAGTGTATGCTCGAA-3′ and 5′-TACTCGCTCGTCTTCCAGGT-3′, for Rap1B 5′-GGTCACAAGGCCTAAGTTGC-3′ and 5′-CATTTGGCCACCTCAAAAGT-3′, for EPAC1 5′-GCAGTCCTGCTCTTTGAACC-3′ and 5′-CTGCTTGTCCACACGAAGAA-3′, and for EPAC2 5′-CATGAGGGGAACAAGACGTT-3′ and 5′-TCTATGGTCGACGAGGCTCT-3′.

The qRT-PCR samples were prepared in a 20-$\mu$l mixture composed of forward and reverse primers at 2 $\mu$M and 5 $\mu$l of the Power SYBR Green PCR master mix. The qRT-PCR was performed in a CFX384 Real-time system C1000 thermal cycler (Bio-Rad). After 39 cycles of PCR, the average threshold cycle ($C_t$) values from triplicate qRT-PCR experiments were normalized against the average $C_t$ values of Scramble siRNA $\beta$-actin and the relative mRNA was quantified using the $\Delta\Delta C_t$ method.

*Author contributions*—C. J. R. helped design all experiments and contributed to all studies presented and authored manuscript. X. L. contributed to measures of cell resistance. C. M. L. contributed to all *in vivo* studies. D. A. A. designed and oversaw all studies and authored the manuscript.

## References


1. Runkle, E. A., and Antonetti, D. A. (2011) The blood-retinal barrier: structure and functional significance. *Methods Mol. Biol.* **686,** 133–148 CrossRef Medline
2. D'Atri, F., and Citi, S. (2002) Molecular complexity of vertebrate tight junctions (review). *Mol. Membr. Biol.* **19,** 103–112 CrossRef Medline
3. van Meer, G., and Simons, K. (1986) The function of tight junctions in maintaining differences in lipid composition between the apical and the basolateral cell surface domains of MDCK cells. *EMBO J.* **5,** 1455–1464 Medline
4. Klaassen, I., Van Noorden, C. J., and Schlingemann, R. O. (2013) Molecular basis of the inner blood-retinal barrier and its breakdown in diabetic macular edema and other pathological conditions. *Prog. Retin Eye Res.* **34,** 19–48 CrossRef Medline
5. Stamatovic, S. M., Johnson, A. M., Keep, R. F., and Andjelkovic, A. V. (2016) Junctional proteins of the blood-brain barrier: new insights into function and dysfunction. *Tissue Barriers* **4,** e1154641 CrossRef Medline
6. Frey, T., and Antonetti, D. A. (2011) Alterations to the blood-retinal barrier in diabetes: cytokines and reactive oxygen species. *Antioxid. Redox Signal.* **15,** 1271–1284 CrossRef Medline
7. Sundstrom, J. M., et al. (2009) Identification and analysis of occludin phosphosites: a combined mass spectrometry and bioinformatics approach. *J. Proteome Res.* **8,** 808–817 CrossRef Medline
8. Aveleira, C. A., Lin, C. M., Abcouwer, S. F., Amrósio, A. F., and Antonetti, D. A. (2010) TNF-$\alpha$ signals through PKC$\zeta$/NF-$\kappa$B to alter the tight junction complex and increase retinal endothelial cell permeability. *Diabetes* **59,** 2872–2882 CrossRef Medline
9. Simó, R., Sundstrom, J. M., and Antonetti, D. A. (2014) Ocular Anti-VEGF therapy for diabetic retinopathy: the role of VEGF in the pathogenesis of diabetic retinopathy. *Diabetes Care* **37,** 893–899 CrossRef Medline
10. He, P., Zeng, M., and Curry, F. E. (2000) Dominant role of cAMP in regulation of microvessel permeability. *Am. J. Physiol. Heart Circ Physiol.* **278,** H1124–1133 Medline
11. Adamson, R. H., Liu, B., Fry, G. N., Rubin, L. L., and Curry, F. E. (1998) Microvascular permeability and number of tight junctions are modulated by cAMP. *Am. J. Physiol.* **274,** H1885-H1194
12. de Rooij, J., Zwartkruis, F. J., Verheijen, M. H., Cool, R. H., and Nijman, S. M., and Wittinghofer, A., and Bos, J. L. (1998) Epac is a Rap1 guanine-nucleotide-exchange factor directly activated by cyclic AMP. *Nature* **396,** 474–477 CrossRef Medline
13. de Rooij, J., Rehmann, H., van Triest, M., Cool, R. H., Willinghofer, A., and Bos, J. L. (2000) Mechanism of regulation of the Epac family of cAMP-dependent RapGEFs. *J. Biol. Chem.* **275,** 20829–20836 Medline
14. Kawasaki, H., Springett, G. M., Mochizuki, N., Toki, S., Nakaya, M., Matsuda, M., Housman, D. E., and Graybiel, A. M. (1998) A family of cAMP-binding proteins that directly activate Rap1. *Science* **282,** 2275–2279 CrossRef Medline
15. Rousseau-Merck, M. F., Pizon, V., Tavitian, A., and Berger, R. (1990) Chromosome mapping of the human RAS-related RAP1A, RAP1B, and RAP2 genes to chromosomes 1p12-p13, 12q14, and 13q34, respectively. *Cytogenet. Cell Genet.* **53,** 2–4 CrossRef Medline
16. van Dam, T. J., Bos, J. L., and Snel, B. (2011) Evolution of the Ras-like small GTPases and their regulators. *Small GTPases* **2,** 4–16 CrossRef Medline
17. Bos, J. L., de Rooij, J., and Reedquist, K. A. (2001) Rap1 signalling: adhering to new models. *Nat. Rev. Mol. Cell Biol.* **2,** 369–377 CrossRef Medline
18. Bos, J. L. (1997) Ras-like GTPases. *Biochim. Biophys. Acta* **1333,** M19–31 Medline

19. Chrzanowska-Wodnicka, M., White, G. C., 2nd, Quilliam, L. A., and Whitehead, K. J. (2015) Small GTPase Rap1 is essential for mouse development and formation of functional vasculature. *PLoS ONE* **10,** e0145689 CrossRef Medline
20. Chrzanowska-Wodnicka, M., Smyth, S. S., Schoenwaelder, S. M., Fischer, T. H., and White, G. C., 2nd. (2005) Rap1b is required for normal platelet function and hemostasis in mice. *J. Clin. Invest.* **115,** 680–687
21. Kooistra, M. R., Dube, N., and Bos, J. L. (2007) Rap1: a key regulator in cell-cell junction formation. *J. Cell Sci.* **120,** 17–22
22. Fukuhara, S., Sakurai, A., Sano, H., Yamagishi, A., Somekawa, S., Takakura, N., Saito, Y., Kangawa, K., and Mochizuki, N. (2005) Cyclic AMP potentiates vascular endothelial cadherin-mediated cell-cell contact to enhance endothelial barrier function through an Epac-Rap1 signaling pathway. *Mol. Cell Biol.* **25,** 136–146 CrossRef Medline
23. Baumer, Y., Drenckhahn, D., and Waschke, J. (2008) cAMP induced Rac 1-mediated cytoskeletal reorganization in microvascular endothelium. *Histochem. Cell Biol.* **129,** 765–778 CrossRef Medline
24. Cullere, X., Shaw, S. K., Andersson, L., Hirahashi, J., Luscinskas, F. W., and Mayadas, T. N. (2005) Regulation of vascular endothelial barrier function by Epac, a cAMP-activated exchange factor for Rap GTPase. *Blood* **105,** 1950–1955 CrossRef Medline
25. Kooistra, M. R., Corada, M., Dejana, E., and Bos, J. L. (2005) Epac1 regulates integrity of endothelial cell junctions through VE-cadherin. *FEBS Lett.* **579,** 4966–4972 CrossRef Medline
26. Adamson, R. H., Ly, J. C., Sarai, R. K., Lenz, J. F., Altangerel, A., Drenckhahn, D., and Curry, F. E. (2008) Epac/Rap1 pathway regulates microvascular hyperpermeability induced by PAF in rat mesentery. *Am. J. Physiol. Heart Circ. Physiol.* **294,** H1188–1196 Medline
27. Muthusamy, A., Lin, C. M., Shanmugam, S., Lindner, H. M., Abcouwer, S. F., and Antonetti, D. A. (2014) Ischemia-reperfusion injury induces occludin phosphorylation/ubiquitination and retinal vascular permeability in a VEGFR-2-dependent manner. *J. Cereb. Blood Flow Metab.* **34,** 522–531 CrossRef Medline
28. Wittchen, E. S., Nishimura, E., McCloskey, M., Wang, H., Quilliam, L. A., Chrzanowska-Wodnicka, M., and Hartnett, M. E. (2013) Rap1 GTPase activation and barrier enhancement in rpe inhibits choroidal neovascularization *in vivo*. *PLoS ONE* **8,** e73070 Medline
29. Enserink, J. M., Christensen, A. E., de Rooij, J., van Triest, M., Schwede, F., Genieser, H. G., Døskeland, S. O., Blank, J. L., and Bos, J. L. (2002) A novel Epac-specific cAMP analogue demonstrates independent regulation of Rap1 and ERK. *Nat. Cell Biol.* **4,** 901–906 CrossRef Medline
30. Harhaj, N. S., Felinski, E. A., Wolpert, E. B., Sundstrom, J. M., Gardner, T. W., and Antonetti, D. A. (2006) VEGF activation of protein kinase C stimulates occludin phosphorylation and contributes to endothelial permeability. *Invest. Ophthalmol. Vis. Sci.* **47,** 5106–5115 CrossRef Medline
31. Bos, J. L. (2003) Epac: a new cAMP target and new avenues in cAMP research. *Nat. Rev. Mol. Cell Biol.* **4,** 733–738 CrossRef Medline
32. Roberts, O. L., and Dart, C. (2014) cAMP signalling in the vasculature: the role of Epac (exchange protein directly activated by cAMP). *Biochem. Soc. Trans.* **42,** 89–97 CrossRef Medline
33. Citalán-Madrid, A. F., García-Ponce, A., Vargas-Robles, H., Betanozos, A., and Schnoor, M. (2013) Small GTPases of the Ras superfamily regulate intestinal epithelial homeostasis and barrier function via common and unique mechanisms. *Tissue Barriers* **1,** e26938 CrossRef Medline
34. Sehrawat, S., Cullere, X., Patel, S., Italiano, J., Jr., and Mayadas, T. N. (2008) Role of Epac1, an exchange factor for Rap GTPases, in endothelial microtubule dynamics and barrier function. *Mol. Biol. Cell* **19,** 1261–1270 Medline
35. Whitaker, C. M., and Cooper, N. G. (2010) Differential distribution of exchange proteins directly activated by cyclic AMP within the adult rat retina. *Neuroscience* **165,** 955–967 CrossRef Medline
36. Penzes, P., Woolfrey, K. M., and Srivastava, D. P. (2011) Epac2-mediated dendritic spine remodeling: implications for disease. *Mol. Cell Neurosci.* **46,** 368–380 CrossRef Medline
37. Liu, J., Yeung, P. K., Chen, L., Lo, A. C., Chung, S. S., and Chung, S. K. (2015) Epac2-deficiency leads to more severe retinal swelling, glial reactivity and oxidative stress in transient middle cerebral artery occlusion induced ischemic retinopathy. *Sci. China Life Sci.* **58,** 521–530 CrossRef Medline
38. Chrzanowska-Wodnicka, M., Kraus, A. E., Gale, D., White, G. C., 2nd, and Vansluys, J. (2008) Defective angiogenesis, endothelial migration, proliferation, and MAPK signaling in Rap1b-deficient mice. *Blood* **111,** 2647–2656 CrossRef Medline
39. Li, Y., Yan, J., De, P., Chang, H. C., Yamuchi, A., Christopherson, K. W., 2nd, Paranavitana, N. C., Peng, X., Kim, C., Munugalavadla, V., Munugulavadla, V., Kapur, R., Chen, H., Shou, W., Staone, J. C., *et al.* (2007) Rap1a null mice have altered myeloid cell functions suggesting distinct roles for the closely related Rap1a and 1b proteins. *J. Immunol.* **179,** 8322–8331 CrossRef Medline
40. Duchniewicz, M., Zemojtel, T., Kolanczyk, M., Grossmann, S., Scheele, J. S., and Zwartkruis, F. J. (2006) Rap1A-deficient T and B cells show impaired integrin-mediated cell adhesion. *Mol. Cell. Biol.* **26,** 643–653 CrossRef Medline
41. Boettner, B., and Van Aelst, L. (2009) Control of cell adhesion dynamics by Rap1 signaling. *Curr. Opin. Cell Biol.* **21,** 684–693 CrossRef Medline
42. Wilson, C. W., and Ye, W. (2014) Regulation of vascular endothelial junction stability and remodeling through Rap1-Rasip1 signaling. *Cell Adh. Migr.* **8,** 76–83 CrossRef Medline
43. Glading, A., Han, J., Stockton, R. A., and Ginsberg, M. H. (2007) KRIT-1/CCM1 is a Rap1 effector that regulates endothelial cell cell junctions. *J. Cell Biol.* **179,** 247–254 CrossRef Medline
44. Birukova, A. A., Tian, X., Tian, Y., Higginbotham, K., and Birukov, K. G. (2013) Rap-afadin axis in control of Rho signaling and endothelial barrier recovery. *Mol. Biol. Cell* **24,** 2678–2688 CrossRef Medline
45. Arita, R., Hata, Y., Nakao, S., Kita, T., Miura, M., Kawahara, S., Zandi, S., Almulki, L., Tayyari, F., Shimokawa, H., Hafezi-Moghadam, A., and Ishibashi, T. (2009) Rho kinase inhibition by fasudil ameliorates diabetes-induced microvascular damage. *Diabetes* **58,** 215–226 CrossRef Medline
46. van Buul, J. D., Geerts, D., and Huveneers, S. (2014) Rho GAPs and GEFs: controling switches in endothelial cell adhesion. *Cell Adh. Migr.* **8,** 108–124 CrossRef Medline
47. Post, A., Pannekoek, W. J., Ross, S. H., Verlaan, I., Brouwer, P. M., and Bos, J. L. (2013) Rasip1 mediates Rap1 regulation of Rho in endothelial barrier function through ArhGAP29. *Proc. Natl. Acad. Sci. U.S.A.* **110,** 11427–11432 CrossRef Medline
48. de Kreuk, B. J., Gingras, A. R., Knight, J. D., Liu, J. J., Gingras, A. C., and Ginsberg, M. H. (2016) Heart of glass anchors Rasip1 at endothelial cell-cell junctions to support vascular integrity. *Elife* **5,** e11394 CrossRef Medline
49. Mitin, N.Y., Ramocki, M. B., Zullo, A. J., Der, C. J., Konieczny, S. F., and Taparowsky, E. J. (2004) Identification and characterization of rain, a novel Ras-interacting protein with a unique subcellular localization. *J. Biol. Chem.* **279,** 22353–22361 CrossRef Medline
50. Wilson, C. W., Parker, L. H., Hall, C. J., Smyczek, T., Mak, J., Crow, A., Posthuma, G., De Maziere, A., Sagolla, M., Chalouni, C., Vitorino, P., Roose-Girma, M., Warming, S., Klumperman, J., Crosier, P. S., and Ye, W. (2013) Rasip1 regulates vertebrate vascular endothelial junction stability through Epac1-Rap1 signaling. *Blood* **122,** 3678–3690 CrossRef Medline
51. Ramos, C. J., and Antonetti, D. A. (2017) The role of small GTPases and EPAC-Rap signaling in the regulation of the blood-brain and blood-retinal barriers. *Tissue Barriers* **5,** e1339768 CrossRef Medline
52. Wittchen, E. S., and Hartnett, M. E. (2011) The small GTPase Rap1 is a novel regulator of RPE cell barrier function. *Invest. Ophthalmol. Vis. Sci.* **52,** 7455–7463 CrossRef Medline
53. Yuan, Z., Zhang, W., and Tan, W. (2013) A labile pool of IQGAP1 disassembles endothelial adherens junctions. *Int. J. Mol. Sci.* **14,** 13377–13390 CrossRef Medline
54. Tian, Y., Gawlak, G., Shah, A. S., Higgenbotham, K., Tien, X, Kawasaki, Y., Akiyama, T., Sacks, D. B., and Birukova, A. A. (2015) Hepatocyte growth factor-induced Asef-IQGAP1 complex controls cytoskeletal remodeling and endothelial barrier. *J. Biol. Chem.* **290,** 4097–4109 CrossRef Medline
55. Wang, H., Han, X., Bretz, C. A., Becker, S., Gambhir, D., Smith, G. W., Samulski, R. J., Wittchen, E. S., Quilliam, L. A., Chrzanowska-Wodnicka, M., and Hartnett, M. E. (2016) Retinal pigment epithelial cell expression of

active Rap 1a by scAAV2 inhibits choroidal neovascularization. *Mol. Ther. Methods Clin. Dev.* **3,** 16056 CrossRef Medline

56. Cook, S. J., Rubinfeld, B., Albert, I., and McCormick, F. (1993) RapV12 antagonizes Ras-dependent activation of ERK1 and ERK2 by LPA and EGF in Rat-1 fibroblasts. *EMBO J.* **12,** 3475–3485 Medline
57. Roskoski, R., Jr. (2012) ERK1/2 MAP kinases: structure, function, and regulation. *Pharmacol. Res.* **66,** 105–143 Medline
58. Murakami, T., Felinski, E. A., and Antonetti, D. A. (2009) Occludin phosphorylation and ubiquitination regulate tight junction trafficking and vascular endothelial growth factor-induced permeability. *J. Biol. Chem.* **284,** 21036–21046 CrossRef Medline
59. Murakami, T., Frey, T., Lin, C., and Antonetti, D. A. (2012) Protein kinase C$\beta$ phosphorylates occludin regulating tight junction trafficking in vascular endothelial growth factor-induced permeability *in vivo*. *Diabetes* **61,** 1573–1583 CrossRef Medline
60. Titchenell, P. M., Lin, C. M., Keil, J. M., Sundstrom, J. M., Smith, C. D., and Antonetti, D. A. (2012) Novel atypical PKC inhibitors prevent vascular endothelial growth factor-induced blood-retinal barrier dysfunction. *Biochem. J.* **446,** 455–467 CrossRef Medline
61. Antonetti, D. A., and Wolpert, E. B. (2003) Isolation and characterization of retinal endothelial cells. *Methods Mol. Med.* **89,** 365–374 CrossRef Medline
62. DeMaio, L., Antonetti, D. A., Scaduto, R. C., Jr., Gardner, T. W., and Tarbell, J. M. (2004) VEGF increases paracellular transport without altering the solvent-drag reflection coefficient. *Microvasc. Res.* **68,** 295–302 Medline